Research Article

Analytical and Experimental Vibration of Sandwich Beams Having Various Boundary Conditions

Eshagh F. Joubaneh (ID)**,[1] Oumar R. Barry** (ID)**,[1,2] and Hesham E. Tanbour[1]**

[1]*College of Engineering and Science, Central Michigan University, 1200 S. Franklin St, Mount Pleasant, MI 48859, USA*
[2]*Department of Mechanical Engineering, Virginia Tech, 635 Prices Fork Road, Blacksburg, VA 2406, USA*

Correspondence should be addressed to Oumar R. Barry; barry1o@cmich.edu

Generalized differential quadrature (GDQ) method is used to analyze the vibration of sandwich beams with different boundary conditions. The equations of motion of the sandwich beam are derived using higher-order sandwich panel theory (HSAPT). Seven partial differential equations of motions are obtained through the use of Hamilton's principle. The GDQ method is utilized to solve the equations of motion. Experiments are conducted to validate the proposed theory. The results from the analytical model are also compared to those from the literature and finite element method (FEM). Parametric studies are conducted to investigate the effects of different parameters on the natural frequency and response of the sandwich beam under various boundary conditions.

1. Introduction

Many engineering applications in aerospace, aeronautics, and robotics use multibody systems that consist of flexible appendages containing sandwich panels. These appendages experience large deflections due to vibration excitations. Sandwich panel structures with soft cores made of foam or low strength honeycomb, like aramid or nomex, are used in various industrial applications. They consist of two composite or metallic layers that are separated by a thick and lightweight core. The types of cores in sandwich beam can vary from honeycomb, web core, and balsa wood to foamed polymer. Such configurations in sandwich panels result in high stiffness, light weight characteristics, and high energy absorption capability. These kinds of properties make sandwich structures very useful in aerospace application. Herrmann et al. gave a brief overview on sandwich beam, explaining the importance of sandwich panels in the aerospace industry [1]. Vinson also reviewed the advantages of sandwich beam construction and its role in many applications [2].

The behavior of sandwich panels can be described using various theories based on the type of core. In the analysis of sandwich panels with very rigid cores, it is a common practice to neglect the transverse deformation of the core. Several authors have investigated these types of sandwich panels. An early theory of sandwich structures, known as the first-order shear deformation theory (FSDT), employs the plate theory by taking the shear rigidity of the core into account but assumes that the longitudinal deformation is linear in the thickness coordinate and that the core is infinitely rigid in the transverse direction. Although this model is simple, the assumptions made are validated by the fact that the sandwich core is statically loaded and stiff in the thickness coordinate.

In reality, the cores of modern sandwich panels are flexible in all directions. Hohe et al. acknowledged this phenomenon by investigating the effect of the transverse compressibility of the core of sandwich beams on the transient dynamic response of structural sandwich panels under rapid loading conditions [3]. Many modified theories take into consideration different assumptions to more effectively model the stress, strain, and displacement distributions along the thickness coordinate. Among the modified theories are two different higher-order sandwich panel theory (HSAPT)

models for sandwich structures. The first model is HSAPT (mixed) in which the displacements of the face sheets along with the shear stresses in the cores are considered to be unknown. Using various computational models, Frostig and Baruch investigated the free vibration of unidirectional sandwich panels of two core types, compressible and incompressible, using the HSAPT (mixed) model [4]. Frostig et al. also studied the behavior of sandwich panels using HSAPT (mixed) for compressible cores while neglecting in-plane stresses [5]. The HSAPT approach has also been used in other investigations [6–8].

The second model is HSAPT (displacement), which assumes cubic longitudinal displacement and quadratic vertical displacement through the thickness of the sandwich beam. The formulation of this model considers shear strain instead of shear stress. Regardless of axial stress in the core and according to the static equilibrium equation, the second model will consider a constant shear distribution within the core thickness. This type of approximation for sandwich beam construction with a soft core is appropriate for static problems. Experimental investigations have shown that HSAPT accurately predicts displacements and axial strain at the surface, points of support, and regions of concentrated loading. In certain regions of the core, using HSAPT, results are acceptable approximations for shear stress and axial strain values through thickness distributions that are away from points of support and areas of concentrated loading. In contrast, obtaining the same values in regions of the core adjacent to concentrated loading and points of support using HSAPT yields inaccurate approximations of the same values mentioned previously. Since axial stress through the length of the core in HSAPT is neglected, this theory can be used for the study of composite beams and composite plates with soft cores possessing only lateral stress. Frostig et al. studied the free vibration of a unidirectional sandwich panel, which consists of compressible and incompressible core by using various computational models [10]. His study also included both displacement and mix HSAPT formulation.

Different methods can be used to solve equations of motion of HSAPT models. The most common methods are dynamic stiffness method (DSM) and GDQ method. Damanpack and Khalili investigated the higher-order free vibration of sandwich beams with flexible cores using DSM [11]. Tornabene and Viola examined general higher-order theories of doubly curved laminated composite shells and panels using the local GDQ method [15]. Hong et al. examined thermal induced vibration of a thermal sleeve using GDQ method, which was used to obtain numerical results of two-layer cross-ply laminated tubes under thermal vibration [16]. The classical finite element method has also been used in numerous works to examine the vibration of sandwich beam [17–21]. Similar to the FEM method, the quadrature element method (QEM) has also been examined by numerous investigators to study sandwich structures [13, 14, 22–25]. It should be noted that the GDQ method is much accurate and computationally less intensive than the classical finite element method [26]. This makes the GDQ method more appealing than other methods.
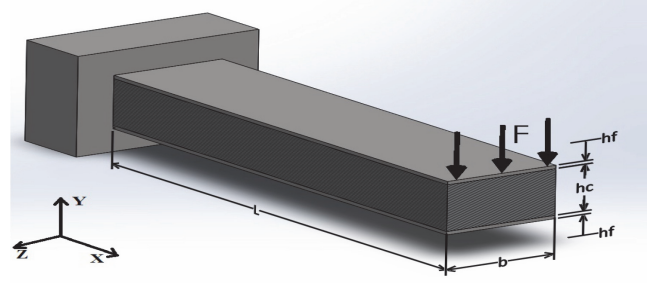

Figure 1: Geometry of sandwich beam.

The GDQ method is adopted in this paper. The objective is to (1) show that HSAPT displacement based model is sufficient for predicting the dynamic behavior of a sandwich beam with soft core under various boundary conditions; (2) conduct experiments to validate the proposed formulation; (3) compare the performance of the GDQ to that of QEM, HQEM, and FEM ABAQUS for a sandwich beam under various boundary conditions; and (4) carry out forced vibration analyses to determine the effect of key design variables on the frequency response curves. To this end, the governing partial differential equations of motion are derived using Hamilton's principle and then the GDQ method is employed to reduce the partial differential equations to ordinary differential equations. Natural frequencies and vibration responses obtained from the analytical model are compared to results from the literature. In addition, finite element analyses are conducted using SolidWorks software to assess the validity of the obtained analytical solutions. Experiments were also performed on sandwich beams with different thicknesses and the results were compared to those obtained using the GDQ method. Parametric studies are carried out to study the effects of various parameters on the natural frequency and response of different sandwich beams.

2. Derivation of the Governing Equations

Figure 1 depicts a schematic of a cantilever sandwich beam, with length L and width b. This beam is composed of three layers: two thin stiff face sheets with thickness h_f and a thick soft core with thickness h_c.

The general assumptions for the derivation of the governing equation of motion are as follows [11]:

 (i) All deformations and strains are very small.

 (ii) The face sheets and the core of the beam are made of isotropic and homogeneous materials.

 (iii) The sandwich beam is assumed to be symmetric.

 (iv) Transverse normal strains are negligible in the face sheets.

 (v) There is no slippage between layers.

 (vi) The face sheets are modeled by Euler-Bernoulli beam theory and the core is modeled using 2D elasticity theory.

It should be noted that the core is more soft through thickness in comparison with the face sheets and the normal stress of the core is negligible. The axial and transverse displacements of a point on the middle of the top face sheet are $u_t(x,t)$ and $w_t(x,t)$, respectively. The transverse and axial displacements of a point on the middle of the bottom face sheets are $u_b(x,t)$ and $w_b(x,t)$, respectively. The axial and transverse displacements of a point on the middle of the core layer are $u_c(x,t)$ and $w_c(x,t)$, respectively. φ_1 is the slope at the centroid of the core; φ_2 and φ_3 are unknown in-plane rotations of the core. ψ_1 and ψ_2 are unknown transverse rotation of the core. The displacement field for the sandwich beam can be expressed as

$$X : \begin{cases} u_t - yw'_t & -\dfrac{h_f}{2} < y < \dfrac{h_f}{2} \\[2ex] u_c + \varphi_1 y + \varphi_2 y^2 + \varphi_3 y^3 & -\dfrac{h_c}{2} < y < \dfrac{h_c}{2} \\[2ex] u_b - yw'_b & -\dfrac{h_f}{2} < y < \dfrac{h_f}{2} \end{cases}$$

$$Y : \begin{cases} w_t & -\dfrac{h_f}{2} < y < \dfrac{h_f}{2} \\[2ex] w_c + \psi_1 y + \psi_2 y^2 & -\dfrac{h_c}{2} < y < \dfrac{h_c}{2} \\[2ex] w_b & -\dfrac{h_f}{2} < y < \dfrac{h_f}{2} \end{cases} \tag{1}$$

Here X and Y are displacement fields in x and y directions. By using the compatibility conditions given as

$$X : \begin{cases} X^{Core}\left(y = \dfrac{h_c}{2}\right) = X^{Topface}\left(y = -\dfrac{h_f}{2}\right) \\[2ex] X^{Core}\left(y = -\dfrac{h_c}{2}\right) = X^{Bottomface}\left(y = \dfrac{h_f}{2}\right) \end{cases}$$

$$Y : \begin{cases} Y^{Core}\left(y = \dfrac{h_c}{2}\right) = Y^{Topface}\left(y = -\dfrac{h_f}{2}\right) \\[2ex] Y^{Core}\left(y = -\dfrac{h_c}{2}\right) = Y^{Bottomface}\left(y = \dfrac{h_f}{2}\right) \end{cases} \tag{2}$$

the displacement fields becomes

$$X : \begin{cases} u_t - yw'_t & -\dfrac{h_f}{2} < y < \dfrac{h_f}{2} \\[2ex] u_c + \varphi_1 y + \left(u_t + u_b + \dfrac{h_f}{2}w'_t - \dfrac{h_f}{2}w'_b - 2u_c\right)\dfrac{2y^2}{h_c^2} + \left(u_t - u_b + \dfrac{h_f}{2}w'_t + \dfrac{h_f}{2}w'_b - h_c\varphi_1\right)\dfrac{4y^3}{h_c^3} & -\dfrac{h_c}{2} < y < \dfrac{h_c}{2} \\[2ex] u_b - yw'_b & -\dfrac{h_f}{2} < y < \dfrac{h_f}{2} \end{cases}$$

$$Y : \begin{cases} w_t & -\dfrac{h_f}{2} < y < \dfrac{h_f}{2} \\[2ex] w_c + \dfrac{(w_t - w_b)\,y}{h_c} + \dfrac{(w_t + w_b - 2w_c)\,2y^2}{h_c^2} & -\dfrac{h_c}{2} < y < \dfrac{h_c}{2} \\[2ex] w_b & -\dfrac{h_f}{2} < y < \dfrac{h_f}{2} \end{cases} \tag{3}$$

$$Z\,(for\ all\ layers) : 0$$

Here w'_t and w'_b are the rotational displacements of top and bottom face sheets. Z defines the displacement field in z direction, which is assumed to be zero. Potential energy for sandwich beam U is given as

$$U = \dfrac{1}{2}\left(\int_{V_t} E_f \varepsilon_x^2 dV_t + \int_{V_c}\left(E_c \varepsilon_y^2 + G_c \gamma_{xy}^2\right) dV_c + \int_{V_b} E_f \varepsilon_x^2 dV_b\right) \tag{4}$$

Here, E_f and E_c are modulus of elasticity of face sheets and the core, respectively, and G_c is the shear modulus of the core. ε_x and ε_y are normal strains in x and y directions and γ_{xy} is the shear strain of the core. V_t, V_b, and V_c are volume of the top, bottom, and core layers, respectively. A_t, A_b, and A_c are the area of top, bottom, and core layers. By substituting the strain displacement equation (3) in (4), the potential energy becomes [11]

$$U = \dfrac{1}{2}\int_0^L \left\{ \int_{A_t} E_f\left(u'_t - yw''_t\right)^2 dA_t + \int_{A_b} E_f\left(u'_b - yw''_b\right)^2 dA_b + \int_{A_c} E_c\left[(w_t - w_b)\dfrac{1}{h_c} + (w_t + w_b - 2w_c)\dfrac{4y}{h_c^2}\right]^2 dA_c \right.$$

$$\left. + \int_{A_c} G_c\left[(\varphi_1 + w'_c) + \left(u_t + u_b + \dfrac{2h_f + h_c}{4}w'_t - \dfrac{2h_f + h_c}{4}w'_b - 2u_c\right)\dfrac{4y}{h_c^2}dA_c + \int_{A_c}\left(u_t - u_b + \dfrac{3h_f + h_c}{6}w'_t + \dfrac{3h_f + h_c}{6}w'_b - h_c\varphi_1 - \dfrac{h_c}{3}w'_c\right)\dfrac{12y^2}{h_c^3}\right]^2 dA_c \right\} dx \tag{5}$$

The kinetic energy is given as

$$
\begin{aligned}
T = \frac{1}{2} \Bigg(& \int_{V_t} \rho_f \left(\dot{x}_t{}^2 + \dot{y}_t{}^2 \right) dV_t \\
& + \int_{V_b} \rho_f \left(\dot{x}_b{}^2 + \dot{y}_b{}^2 \right) dV_b + \int_{V_c} \rho_c \left(\dot{x}_c{}^2 + \dot{y}_c{}^2 \right) dV_c \Bigg)
\end{aligned}
\tag{6}
$$

where ρ_f is the face sheets density and ρ_c is the core density. $\dot{x}_t$, $\dot{x}_b$, and $\dot{x}_c$ are velocities of top and bottom face sheets and core in x direction. $\dot{y}_t$, $\dot{y}_b$, and $\dot{y}_c$ are velocities of top and bottom face sheets and core in y direction. By substituting the displacement equations into (5) and (6), the governing partial differential equations of motion and boundary conditions can be obtained from Hamilton's principle as

$$
\delta \int_{t_1}^{t_2} (T - U)\, dt = 0
\tag{7}
$$

where δ is the first variation operation and t_1 and t_2 are defined as the time period. The governing equations of motion are obtained by dividing and factoring the coefficients of $\delta u_t, \delta u_b, \delta w_t, \delta w_b, \delta u_c, \delta \varphi, \delta w_c$ in (7). The following equation is one of the seven obtained equations of motion. The rest of the equations are presented in the Appendix.

$$
\begin{aligned}
m_f \left(\ddot{u}_t \right) + m_c \Bigg[& \frac{1}{20} \left(\ddot{u}_t + \ddot{u}_b \right) + \frac{1}{28} \left(\ddot{u}_t - \ddot{u}_b \right) + \frac{1}{15} \ddot{u}_c \\
& + \frac{1}{70} h_c \ddot{\varphi}_1 + \frac{1}{40} h_f \left(\ddot{w}'_t - \ddot{w}'_b \right) + \frac{1}{56} h_f \left(\ddot{w}'_t + \ddot{w}'_b \right) \Bigg] \\
& - E_f A_f u''_t + \frac{G_c A_c}{h_c^2} \Bigg[\frac{4}{3} \left(u_t + u_b \right) + \frac{9}{5} \left(u_t - u_b \right) \\
& - \frac{8}{3} u_c - \frac{4}{5} h_c \varphi_1 + \left(\frac{2}{3} h_f + \frac{1}{3} h_c \right) \left(w'_t - w'_b \right) \\
& + \left(\frac{9}{10} h_f + \frac{3}{10} h_c \right) \left(w'_t + w'_b \right) + \frac{2}{5} h_c w'_c \Bigg] = 0
\end{aligned}
\tag{8}
$$

where m_c is the core's mass, m_f is the surface layers' mass, I_f is the surface moment of inertia, A_c is the core's cross section, and A_f is the surface layers' cross section. $\ddot{u}_t$ and $\ddot{u}_b$ are also the accelerations at the middle of the top and bottom face sheets and $\ddot{u}_c$ is the acceleration at the middle of the core. u''_t defines the variation of normal strain related to middle of the top face sheet in x direction.

3. GDQ Method

The GDQ method is applied in order to discrete the equation of motion and boundary condition along the length of the beam. Applying GDQ method to the equation of motion (see (8)) yields

$$
\begin{aligned}
& \left[m_f + m_c \left(\frac{1}{20} + \frac{1}{28} \right) \right] \sum_{j=1}^{N} C_{ij}^{(0)} \ddot{u}_t \left(x_j \right) \\
& + m_c \left(\frac{1}{20} - \frac{1}{28} \right) \sum_{j=1}^{N} C_{ij}^{(0)} \ddot{u}_b \left(x_j \right) + m_c \left(\frac{1}{15} \right) \\
& \cdot \sum_{j=1}^{N} C_{ij}^{(0)} \ddot{u}_c \left(x_j \right) + m_c h_c \frac{1}{70} \sum_{j=1}^{N} C_{ij}^{(0)} \ddot{\varphi}_1 \left(x_j \right) \\
& + m_c \left(\frac{1}{40} + \frac{1}{56} \right) h_f \sum_{j=1}^{N} C_{ij}^{(1)} \ddot{w}_t \left(x_j \right) \\
& + m_c \left(-\frac{1}{40} + \frac{1}{56} \right) h_f \sum_{j=1}^{N} C_{ij}^{(1)} \ddot{w}_b \left(x_j \right) \\
& - E_f A_f \sum_{j=1}^{N} C_{ij}^{(2)} u_t \left(x_j \right) + \frac{G_c A_c}{h_c^2} \left(\frac{4}{3} + \frac{9}{5} \right) \\
& \cdot \sum_{j=1}^{N} C_{ij}^{(0)} u_t \left(x_j \right) + \frac{G_c A_c}{h_c^2} \left(\frac{4}{3} - \frac{9}{5} \right) \sum_{j=1}^{N} C_{ij}^{(0)} u_b \left(x_j \right) \\
& - \frac{G_c A_c}{h_c^2} \left(\frac{8}{3} \right) \sum_{j=1}^{N} C_{ij}^{(0)} u_c \left(x_j \right) \\
& + \frac{G_c A_c}{h_c^2} \left[\left(\frac{2}{3} h_f + \frac{1}{3} h_c \right) + \left(\frac{9}{10} h_f + \frac{3}{10} h_c \right) \right] \\
& \cdot \sum_{j=1}^{N} C_{ij}^{(1)} w_t \left(x_j \right) \\
& + \frac{G_c A_c}{h_c^2} \left[-\left(\frac{2}{3} h_f + \frac{1}{3} h_c \right) + \left(\frac{9}{10} h_f + \frac{3}{10} h_c \right) \right] \\
& \cdot \sum_{j=1}^{N} C_{ij}^{(1)} w_b \left(x_j \right) + \frac{G_c A_c}{h_c^2} \left(\frac{2}{5} h_c \right) \sum_{j=1}^{N} C_{ij}^{(1)} w_c \left(x_j \right) \\
& - \frac{G_c A_c}{h_c^2} \left(\frac{4}{5} h_c \right) \sum_{j=1}^{N} C_{ij}^{(0)} \varphi_1 \left(x_j \right)
\end{aligned}
\tag{9}
$$

The solution of the system is achieved by employing a local version of the well-known GDQ method. With respect to the global form, this local approach considers localized interpolating basis function. The numerical technique in GDQ is able to evaluate the nth derivative at a generic point of a sufficiently smooth function $f(x)$ as a weighted linear sum of the function values at some chosen grid points in x direction. These grid points can be distributed through the thickness of the sandwich beam too [14].

$$
\frac{d^n f(x)}{dx^n} \left(x_i \right) \cong \sum_{j=1}^{j=N} C_{ij}^{(n)} f \left(x_j \right) \quad \text{for } i = 1, 2 \ldots, N
\tag{10}
$$

where $C_{ij}^{(n)}$ is the weighting coefficient associated with the nth-order derivative and N is the number of grid points in x direction. It should be noted that the GDQ is quite different from QEM and HQEM. GDQ method uses Chebyshev grid points distribution and employs Lagrange function for all displacement fields, namely, u_t, u_b, u_c, φ_1, w_t, w_b, w_c, and φ_1. The QEM, on the other hand, uses expanded Chebyshev grids and employs Hermit functions for w_t, w_b, and w_c and

Lagrange function for displacement fields u_t, u_b, u_c, and φ_1. HQEM, which is an extended version of the QEM, employs nodes on both longitudinal and through the thickness (transverse) directions, whereas the GDQ method and QEM only use nodes in the longitudinal direction. The GDQ method is adopted in this paper; as such, using Lagrange interpolated polynomials for all displacements, the function $f(x)$ can be written as

$$f(x) = \sum_{j=1}^{j=N} \frac{(x-x_1)(x-x_2)\ldots(x-x_{j-1})(x-x_{j+1})\ldots(x-x_N)}{(x_j-x_1)(x_j-x_2)(x_j-x_{j-1})\ldots(x_j-x_N)} f(x_j) \tag{11}$$

Taking the derivative of (11) with respect to x yields

$$f'(x) = \sum_{j=1}^{j=N} \left\{ \frac{(x-x_1)(x-x_2)\ldots(x-x_{j-1})(x-x_{j+1})\ldots(x-x_N)}{(x_j-x_1)(x_j-x_2)(x_j-x_{j-1})\ldots(x_j-x_N)} \right\}' f(x_j) \tag{12}$$

The coefficient of $f(x_j)$ calls $C_{ij}^{(1)}$, which can be written as

$$C_{ij}^{(1)} = \frac{M^{(1)}(x_i)}{(x_i-x_j)M^{(1)}(x_j)}$$
$$C_{ii}^{(1)} = -\sum_{j=1, j\neq i}^{N} C_{ij}^{(1)} \tag{13}$$

where

$$M^{(1)}(x_j) = \prod_{k=1, k\neq j}^{N} (x_j - x_k) \tag{14}$$

The higher-order derivatives are obtained as

$$C_{ij}^{(m)} = m\left[C_{ij}^{(1)}C_{ii}^{(m-1)} - \frac{C_{ij}^{(m-1)}}{x_i-x_j} \right]$$
$$i, j = 1, 2, \ldots, N, \ m = 2, 3, \ldots, N-1, \ i \neq j \tag{15}$$

$$C_{ii}^{(m)} = -\sum_{j=1, j\neq i}^{N} C_{ij}^{(m)}$$

There are also different arrangements of grid points which are used in GDQ method. It has been shown in the literature that using equal spacing sample of grid points gives inaccurate results. Therefore, the Chebyshev-Gauss-Lobatto distribution is employed to discretize the spatial domain as follows [27]:

$$x_i = \frac{L}{2}\left[1 - \cos\left(\frac{i-1}{N-1}\pi\right) \right], \quad i = 1, \ldots, N \tag{16}$$

Other grid distributions such as expanded Chebyshev [13, 14] can also be used.

4. Numerical Results and Discussion

The properties of the sandwich beam used for conducting the numerical simulation are listed in Table 1. Numerical results are presented for the free and forced vibration analyses of sandwich beams with various boundary conditions including cantilever (C-F), clamped-clamped (C-C), simply-simply (S-S), free-free (F-F), and simply-clamped (S-C).

4.1. Free Vibration. To examine the validity of the present formulation, Table 2 compares the results of the GDQ method for the simply supported case to those of [11, 12]. The results show excellent agreement with the closed-form solution employed in [11]. Table 2 also indicates that the GDQ method performs better than the method used in [12]. The validation of the rest of the boundary conditions, namely, C-F, C-C, S-S, F-F, and S-C, is shown in Table 3. The natural frequency of the sandwich beam for GDQ method is compared to those of the QEM, harmonic quadrature element method (HQEM), and finite element method of ABAQUS. The results show very good agreement for all five boundary conditions. In general, it can be observed from Table 3 that the results of the GDQ method and the HQEM are closer to those of ABAQUS than the QEM. This is an indication that the GDQ is more accurate than the QEM. The first two mode shapes for C-F, S-S, and C-C boundary conditions are shown in Figure 2. The results show that the plotted mode shapes are similar to those obtained in [14].

4.2. Forced Vibration. This section discusses the time and frequency responses of the sandwich beam with various boundary conditions. All the numerical simulations in this section are based on a harmonic applied load F at the tip of the sandwich beam defined as $F = 0.4 \times 10^3 \sin(\omega t)$ and the

TABLE 1: Parameters of sandwich beam.

References	E_f (GPa)	G_c (MPa)	ρ_f (kg/m³)	ρ_c (kg/m³)	h_f (mm)	h_c (mm)	b (mm)	L (mm)
[11]	210	22.1	7900	60	1.9	34.8	59.9	260
[12]	36	20.0	4400	52.1	0.5	20.0	20.0	300
[13]	13.6	12.8	1800	58.5	5	19	20	152
Experiment	210	22.1	7900	60	1.9	15 and 25	59.9	260

TABLE 2: The five low natural frequencies for a simply supported sandwich beam (rad/s).

Mode	Present method (GDQ)	Exact [11]	Model (C) [12]
1	2048.46	2048.41	2048.19
2	5189.73	5189.67	5183.37
3	8250.24	8250.19	8224.06
4	11225.32	11225.27	11159.63
5	14139.22	14139.19	14009.12

material property from [11] listed in Table 1. Figure 3 shows the time response of the cantilever sandwich beam for three excitation frequencies, namely, $\omega = 0.1\omega_1$, $\omega = 0.87\omega_1$, and $\omega \simeq 1\omega_1$. Here ω_1 is the first natural frequency of sandwich beam. Beating phenomenon is observed when the excitation frequency is $\omega = 0.87\omega_1$ and resonance phenomenon is demonstrated when the excitation frequency matches the fundamental frequency of the sandwich beam, that is, $\omega \simeq 1\omega_1$. Figure 3 also shows much smaller vibration amplitude when the fundamental frequency is far from the excitation frequency, $\omega = 0.1\omega_1$.

The validation of the forced vibration analysis is demonstrated in Figure 4 by comparing the results of the GDQ method (Case: (a), (c), (e)) to those of SolidWorks simulation (Case: (b), (d), (f)). It should be noted that this figure shows the time response measured at the tip of the cantilever sandwich beam with varying thickness and width. For each case, the cantilever sandwich beam is excited with its corresponding fundamental frequency, since natural frequency changes with beam thickness/width. The results in this figure show very good agreement between the GDQ method and SolidWorks simulations.

It is also observed in Figure 4 that the vibration amplitude decreases with increasing core thickness and/or increasing face sheet thickness. This is expected as increasing thickness increases bending stiffness, thus resulting in lower deflection. Figure 4 also shows the role of the beam width on the time response. The results show that the vibration amplitude decreases with increasing beam width. This is also expected as the width increases with bending stiffness. Although both thickness and width affect the vibration amplitude, only the thickness affects the natural frequency of the beam. This observation is in agreement with literatures [28, 29].

Figures 5, 6, and 7 show the role of geometry parameters on the frequency response curves for cantilever, simply-simply supported, and clamped-clamped boundary conditions, respectively. Similar trends are observed for all three boundary conditions. The frequency response curves are significantly affected by the core and face sheet thicknesses as well as the width of the sandwich beam. Increasing

any of these geometry parameters obviously decreases the vibration amplitude. The peaks corresponding to the excitation frequency change with varying thickness but remain constant with varying width. The natural frequency in general increases with increasing core thickness for all studied boundary conditions. As for the face sheet thickness, the natural frequency can increase or decrease with varying face sheet thickness. The reason for this can be attributed to the core thickness having more effect on the stiffness than the mass, whereas the sheet thickness has similar effect on both mass and stiffness. The beam width shows no effect on the natural frequency for all boundary conditions. This observation is also in agreement with earlier discussion about the role of the beam width on the natural frequency.

5. Experimental Analysis and Discussion

An experiment is conducted to determine the frequency response curve of two cantilever sandwich beams with different core thicknesses. The material properties of the tested sandwich beams are listed in Table 1. A schematic of the experimental setup is depicted in Figure 8. The cantilever beam is installed on a VDL shaker (B & K V830-335-SPA16K) using a head plate and a fixture, both made of aluminum.

To reduce experimental error, the fixture is designed in SolidWorks such that its fundamental frequency is well above the maximum excitation frequency. A signal generated from the controller (Laser USB, 1.4V) is fed to the power amplifier (LSD SPA 16K) and then to the vibration shaker. The signal is fed back to the controller to ensure precise measurement. Two accelerometers (B & K 8325) are employed for input and output measurements. One is placed at the top of the fixture to measure the input acceleration and the other is placed at the tip of the beam to measure the output response. The test is carried out with a constant velocity of 2 mm/s and a sine sweep is performed for a frequency range of 10 to 2000 Hz. Measurements are sent to the data acquisition system through a signal analyzer. The frequency response plots are obtained and the frequencies corresponding to the peaks of these plots are the natural frequencies of the tested sandwich
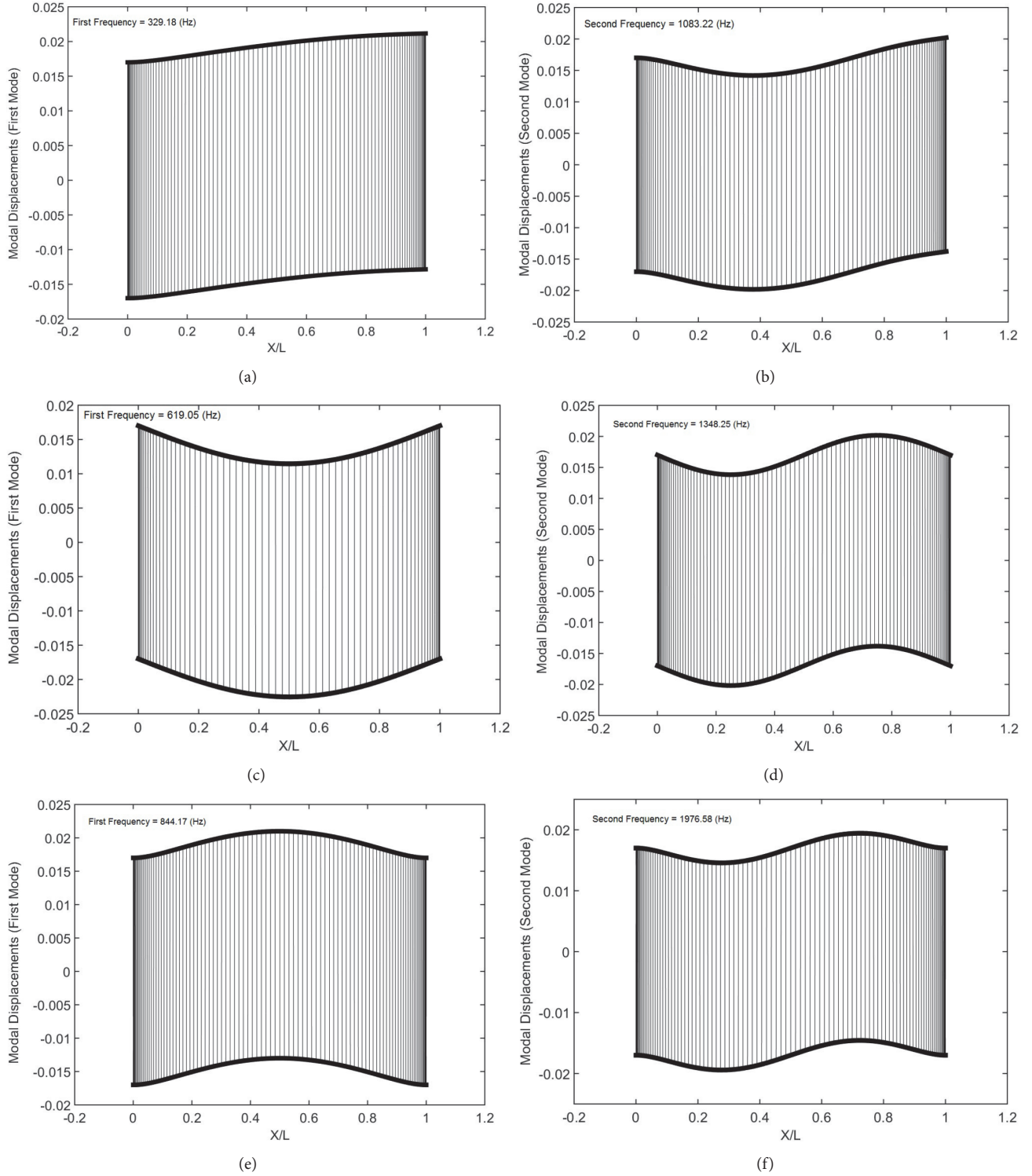
FIGURE 2: The first two mode shapes of sandwich beam with cantilever ((a) and (b)), simply-simply ((c) and (d)), and clamped-clamped ((e) and (f)) supported edges.

beams. The experimental results are shown in Figure 9, which also illustrates the role of the core thickness on the frequency response curve. The results clearly indicate that natural frequency increases with increasing thickness, while vibration response decreases with increasing thickness. This observation is in agreement with the results obtained using the GDQ method. Table 4 compares natural frequencies obtained experimentally and numerically (GDQ method) for
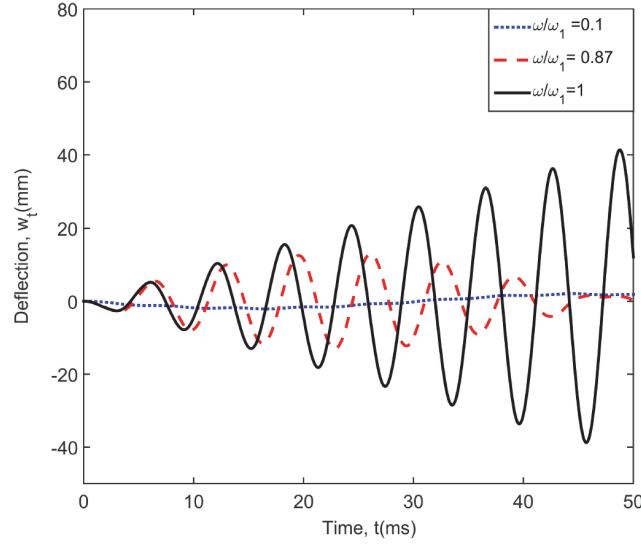
FIGURE 3: Tip deflection of free edge of cantilever sandwich beam (ω_t) for applied frequency $\omega/\omega_1 = 0.1$, $\omega/\omega_1 = 0.87$, and $\omega/\omega_1 \simeq 1$ [9].

TABLE 3: The five low natural frequencies for different boundary conditions (Hz).

BCs	Mode	1	2	3	4	5
C-F	ABAQUS [14]	327.40	1079.1	2138.0	2175.3	2216.4
	GDQ	329.18	1083.22	2152.54	2201.58	2258.15
	QEM [13]	329.66	1088.43	2164.59	2183.78	2225.72
	HQEM (full [M]) [14]	327.82	1082.4	2153.9	2175.9	2217.9
C-C	ABAQUS [14]	839.92	1956.7	2255.6	2702.6	3477.8
	GDQ	844.17	1976.58	2274.56	2709.82	3541.27
	QEM [13]	848.71	1988.13	2262.66	2725.13	3563.96
	HQEM (full [M]) [14]	844.03	1978.1	2257.1	2717.5	3547.5
S-S	ABAQUS [14]	618.56	1349.1	1503.3	2170.4	2358.4
	GDQ	619.05	1348.25	1508.81	2212.64	2413.09
	QEM [13]	622.22	1352.86	1515.45	2176.86	2369.77
	HQEM (full [M]) [14]	618.91	1349.3	1508.2	2171.2	2362.3
F-F	ABAQUS [14]	1290.2	1366.9	2153.7	2169.2	2214.6
	GDQ	1292.10	1366.87	2197.87	2203.86	2245.86
	QEM [13]	1299.19	1372.39	2162.80	2176.40	2225.19
	HQEM (full [M] [14]	1291.8	1367.6	2154.2	2170.1	2215.2
S-C	ABAQUS [14]	715.45	1714.4	2196.4	2514.4	3117.1
	GDQ	717.25	1725.64	2233.9	2541.3	3157.28
	HQEM (full [M]) [14]	717.18	1725.8	2197.5	2521.2	3160.7

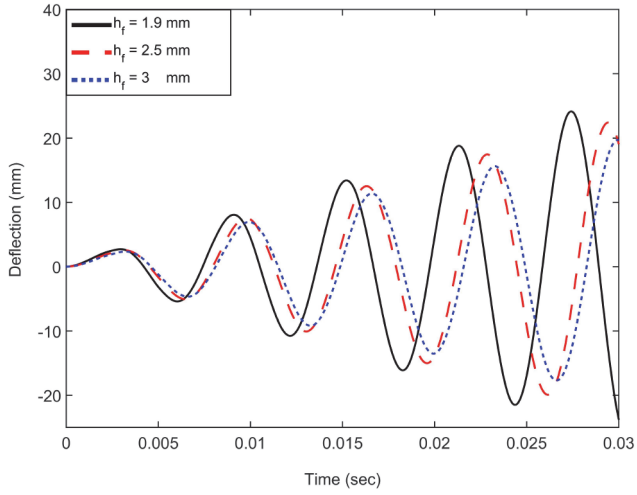TABLE 4: The natural frequencies (Hz) for cantilever beam with two different thicknesses.

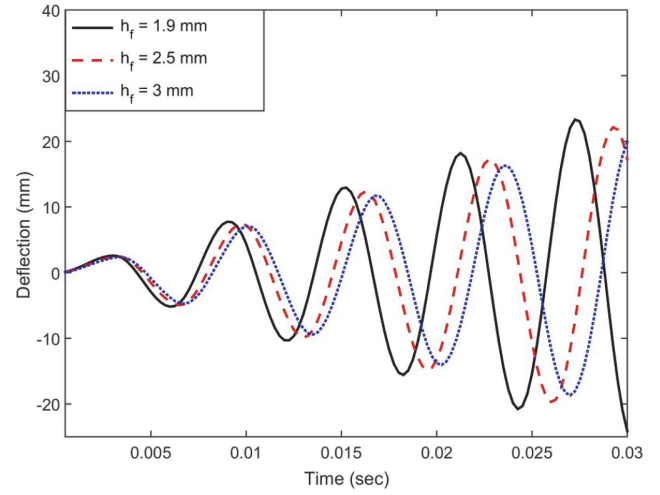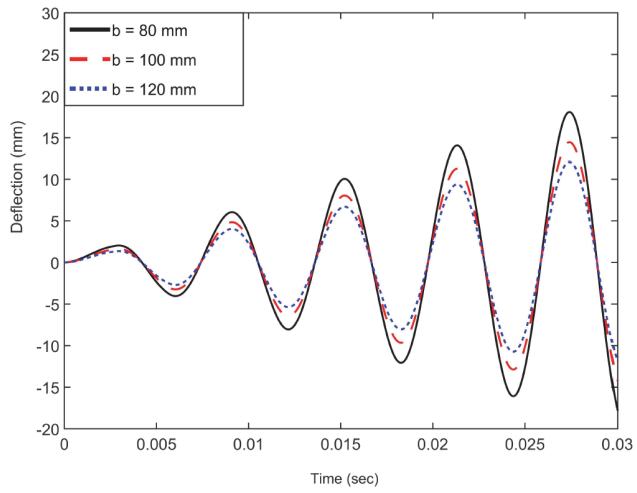| Modes	$h_c = 15$ mm		$h_c = 25$ mm	
	GDQ method	Experiment	GDQ method	Experiment
1	118.00	111.19	143.92	143.02
2	381.00	364.60	452.27	475.21
3	719.84	680.80	821.86	824.33
4	1141.94	1063.50	1261.56	1323.81
5	1675.51	1652.07	1800.17	1772.60
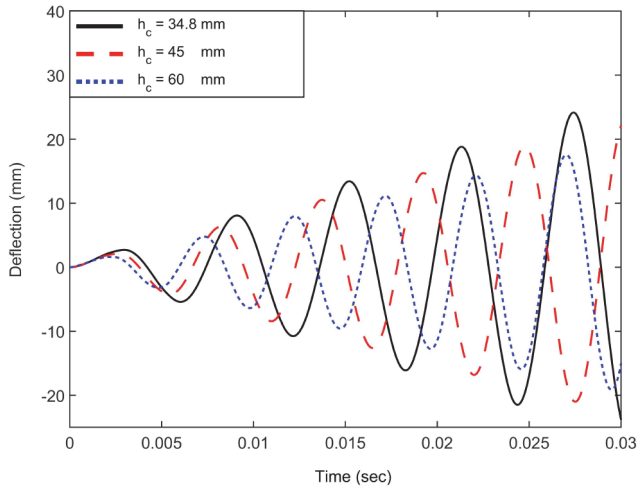
(a) The effect of core by GDQ method
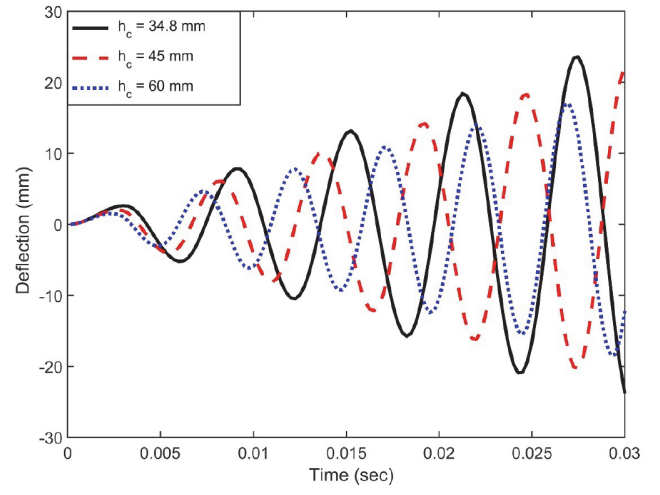
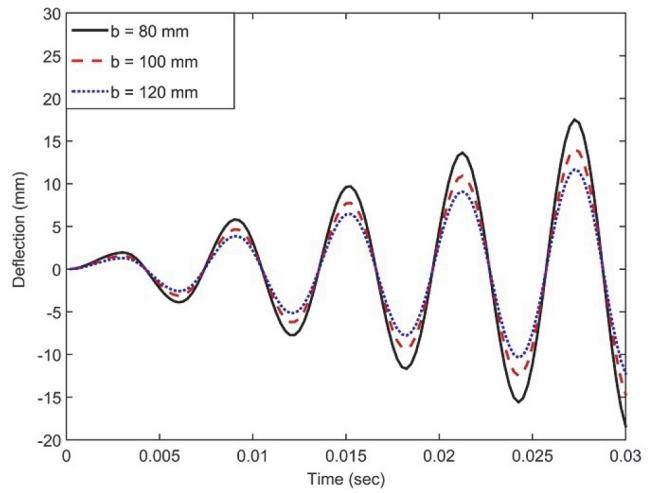(b) The effect of core by SolidWorks

(c) The effect of face sheets by GDQ method

(d) The effect of face sheets by SolidWorks

(e) The effect of width by GDQ method

(f) The effect of width by SolidWorks

FIGURE 4: The effect of geometric parameters on the time response at the tip of the cantilever sandwich beam.
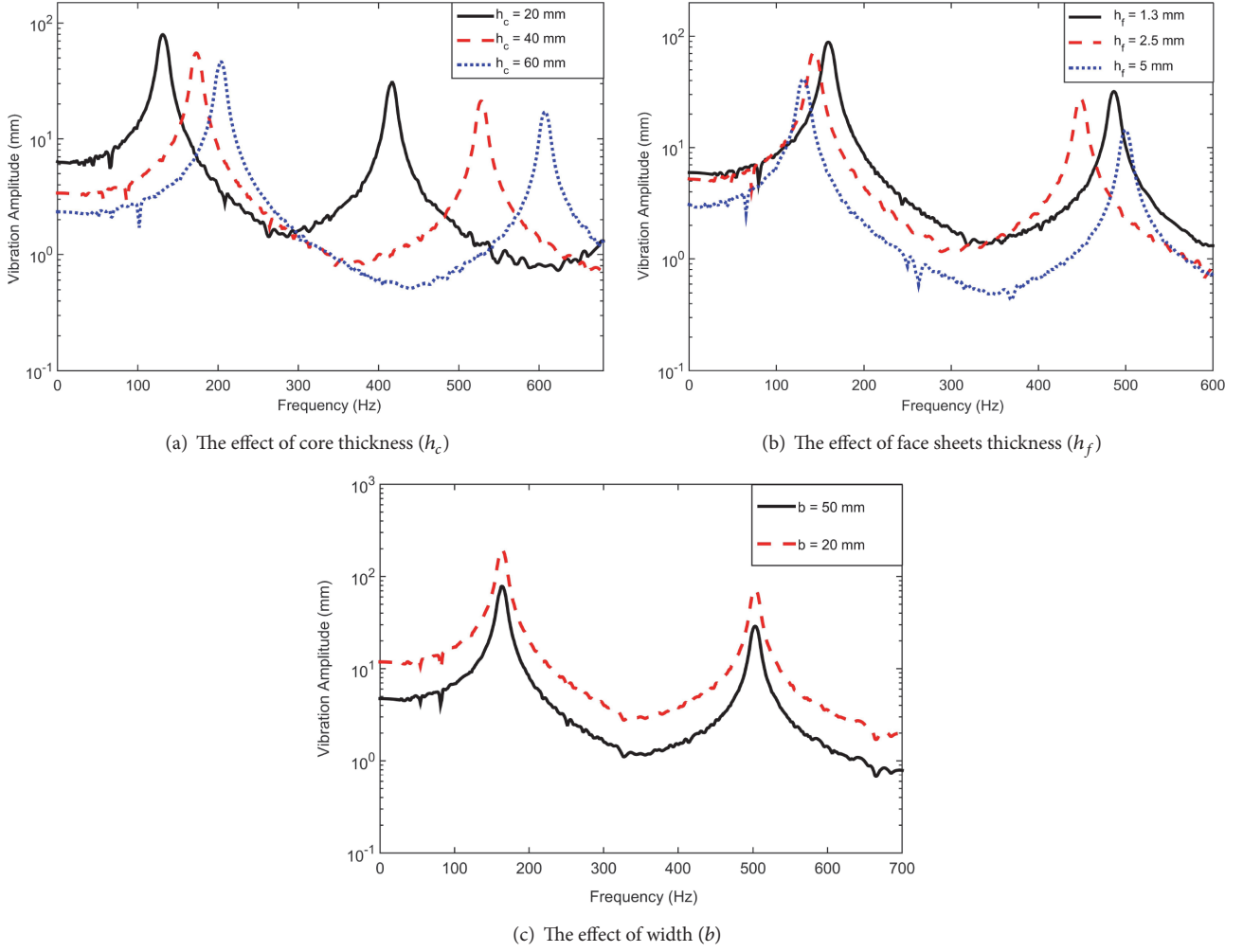
(a) The effect of core thickness (h_c)

(b) The effect of face sheets thickness (h_f)

(c) The effect of width (b)

FIGURE 5: Vibration amplitude at the tip of the cantilever beam with respect to applied frequency.

a core thickness of 15 and 25 mm. The results in this table also show very good agreement. This is also an indication that the present formulation for both free and forced vibration analyses of sandwich beams is accurate.

6. Conclusions

This paper presents the vibration analysis of sandwich beams with various boundary conditions. The governing equations of motion are derived using Hamilton's principle. The GDQ method is utilized for solving the problem. SolidWorks simulation and experimental analyses are conducted to assess the validity of the GDQ method and the results show very good agreement. Parametric studies are conducted to examine the role of geometric properties on the time and frequency response curves. The results indicate that vibration amplitude decreases with increasing both core and face sheet thicknesses, whereas natural frequency increases with increasing core sheet thickness but can increase or decrease with varying face sheet thickness. The results also show that vibration amplitude decreases with increasing beam width, whereas no effect is observed on the natural frequency for

varying the width of the beam. Numerical examples also demonstrate that all studied boundary conditions exhibit similar effect with varying the aforementioned geometric properties. The findings in this paper are anticipated to be appealing to research communities because of the experimental and FEM validation of the GDQ method for the free and forced vibration analyses of sandwich beams under various boundary conditions.

Appendix

The rest of the six equations of motion are given as follows:

$$
m_f \left(\ddot{u}_b \right) + m_c \left[\frac{1}{20} \left(\ddot{u}_t + \ddot{u}_b \right) - \frac{1}{28} \left(\ddot{u}_t - \ddot{u}_b \right) + \frac{1}{15} \ddot{u}_c \right.
$$

$$
- \frac{1}{70} h_c \ddot{\varphi}_1 + \frac{1}{40} h_f \left(\ddot{w}'_t - \ddot{w}'_b \right) - \frac{1}{56} h_f \left(\ddot{w}'_t + \ddot{w}'_b \right) \right]
$$

$$
- E_f A_f u''_b + \frac{G_c A_c}{h_c^2} \left[\frac{4}{3} \left(u_t + u_b \right) - \frac{9}{5} \left(u_t - u_b \right) \right.
$$

$$
- \frac{8}{3} u_c + \frac{4}{5} h_c \varphi_1 + \left(\frac{2}{3} h_f + \frac{1}{3} h_c \right) \left(w'_t - w'_b \right)
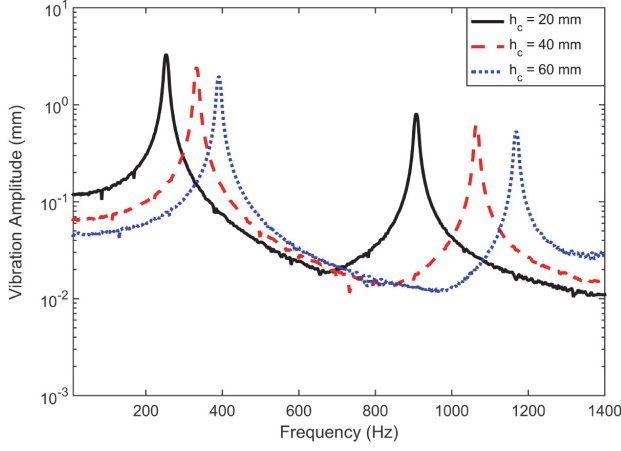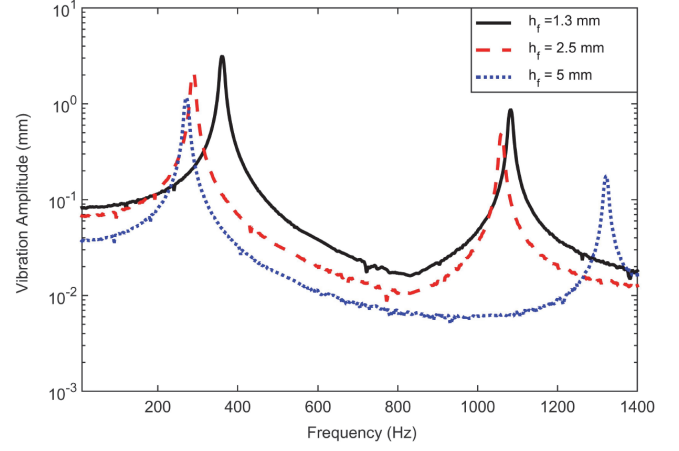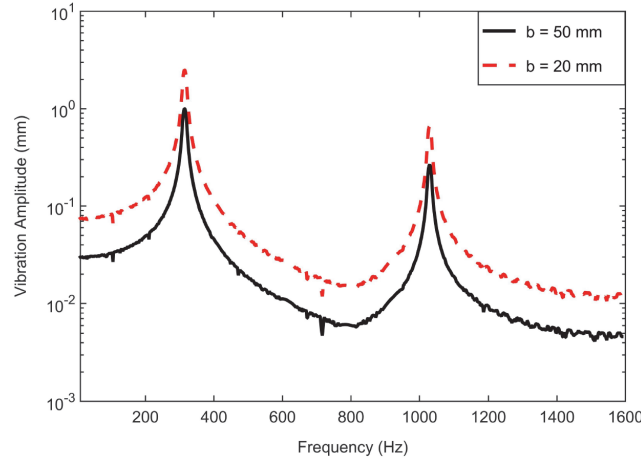$$

(a) The effect of core thickness (h_c)

(b) The effect of face sheets thickness (h_f)

(c) The effect of width (b)

FIGURE 6: Vibration amplitude at the middle of the simply-simply supported edges sandwich beam with respect to applied frequency.

$$-\left(\frac{9}{10}h_f + \frac{3}{10}h_c\right)\left(w'_t + w'_b\right) - \frac{2}{5}h_c w'_c\right] = 0$$

(A.1)

$$m_f\left(\ddot{w}_t - \frac{1}{12}h_f^2 \ddot{w}''_t\right) + m_c\left[-\frac{1}{40}h_f\left(\ddot{u}'_t + \ddot{u}'_b\right)\right.$$

$$-\frac{1}{56}h_f\left(\ddot{u}'_t - \ddot{u}'_b\right) - \frac{1}{30}h_f \ddot{u}'_c - \frac{1}{140}h_c h_f \ddot{\varphi}_1{}'$$

$$-\frac{1}{80}h_f^2\left(\ddot{w}''_t - \ddot{w}''_b\right) + \frac{1}{12}\left(\ddot{w}_t - \ddot{w}_b\right)$$

$$-\frac{1}{112}h_f^2\left(\ddot{w}''_t + \ddot{w}''_b\right) + \frac{1}{20}\left(\ddot{w}_t + \ddot{w}_b\right) + \frac{1}{15}\ddot{w}_c\right]$$

$$+ E_f I_f w''''_t + \frac{G_c A_c}{h_c^2}\left[-\left(\frac{2}{3}h_f + \frac{1}{3}h_c\right)\left(u'_t + u'_b\right)\right.$$

$$-\left(\frac{9}{10}h_f + \frac{3}{10}h_c\right)\left(u'_t - u'_b\right) + \left(\frac{4}{3}h_f + \frac{2}{3}h_c\right)u'_c$$

$$+\left(\frac{2}{5}h_f h_c + \frac{2}{15}h_c^2\right)\left(\varphi'_1\right)$$

$$-\left(\frac{9}{20}h_f^2 + \frac{3}{10}h_c h_f + \frac{1}{20}h_c^2\right)\left(w''_t + w''_b\right)$$

$$-\left(\frac{1}{3}h_f h_c + \frac{1}{3}h_f^2 + \frac{1}{12}h_c^2\right)\left(w''_t - w''_b\right)$$

$$-\left(\frac{1}{5}h_f h_c + \frac{1}{15}h_c^2\right)w''_c\right] + \frac{E_c A_c}{h_c^2}\left[\frac{4}{3}\left(w_t + w_b\right)\right.$$

$$+ \left(w_t - w_b\right) - \frac{8}{3}w_c\right] = 0$$

(A.2)

$$m_f\left(\ddot{w}_b - \frac{1}{12}h_f^2 \ddot{w}''_b\right) + m_c\left[\frac{1}{40}h_f\left(\ddot{u}'_t + \ddot{u}'_b\right)\right.$$

$$-\frac{1}{56}h_f\left(\ddot{u}'_t - \ddot{u}'_b\right) + \frac{1}{30}h_f \ddot{u}'_c - \frac{1}{140}h_c h_f \ddot{\varphi}_1{}'$$

$$+\frac{1}{80}h_f^2\left(\ddot{w}''_t - \ddot{w}''_b\right) - \frac{1}{12}\left(\ddot{w}_t - \ddot{w}_b\right)$$

$$-\frac{1}{112}h_f^2\left(\ddot{w}''_t + \ddot{w}''_b\right) + \frac{1}{20}\left(\ddot{w}_t + \ddot{w}_b\right) + \frac{1}{15}\ddot{w}_c\right]$$

(a) The effect of core thickness (h_c)

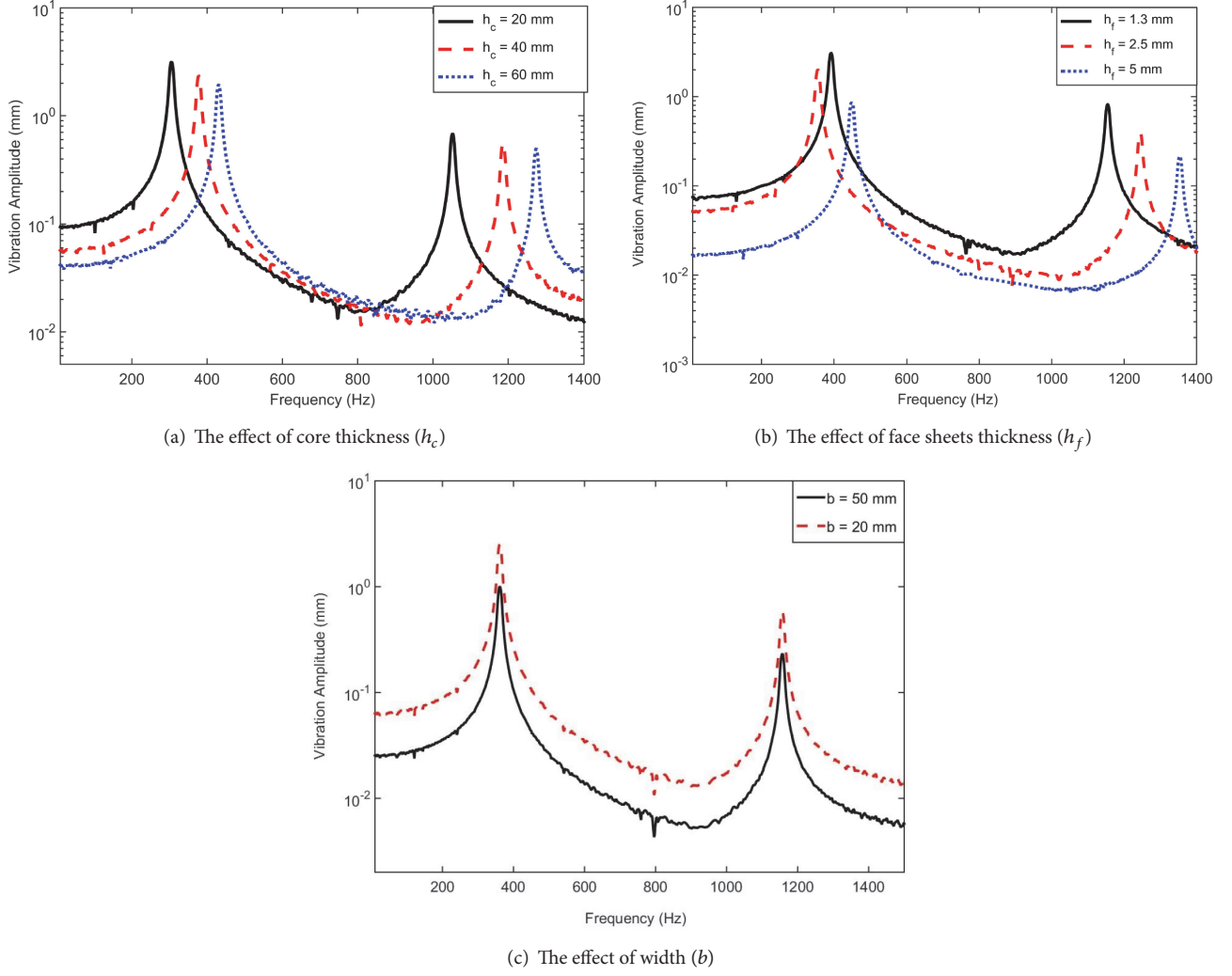(b) The effect of face sheets thickness (h_f)

(c) The effect of width (b)

FIGURE 7: Vibration amplitude at the middle of the clamped-clamped edges sandwich beam with respect to applied frequency.

$$+ E_f I_f w_b'''' + \frac{G_c A_c}{h_c^2} \left[\left(\frac{2}{3}h_f + \frac{1}{3}h_c \right) \left(u_t' + u_b' \right) \right.$$

$$- \left(\frac{9}{10}h_f + \frac{3}{10}h_c \right) \left(u_t' - u_b' \right) - \left(\frac{4}{3}h_f + \frac{2}{3}h_c \right) u_c'$$

$$+ \left(\frac{2}{5}h_f h_c + \frac{2}{15}h_c^2 \right) \left(\varphi_1' \right)$$

$$- \left(\frac{9}{20}h_f^2 + \frac{3}{10}h_c h_f + \frac{1}{20}h_c^2 \right) \left(w_t'' + w_b'' \right)$$

$$+ \left(\frac{1}{3}h_f h_c + \frac{1}{3}h_f^2 + \frac{1}{12}h_c^2 \right) \left(w_t'' - w_b'' \right)$$

$$- \left(\frac{1}{5}h_f h_c + \frac{1}{15}h_c^2 \right) w_c'' \right] + \frac{E_c A_c}{h_c^2} \left[\frac{4}{3} \left(w_t + w_b \right) \right.$$

$$\left. - \left(w_t - w_b \right) - \frac{8}{3} w_c \right] = 0$$

$$\text{(A.3)}$$

$$m_c \left[\frac{8}{15}\ddot{u}_c + \frac{1}{15} \left(\ddot{u}_b + \ddot{u}_t \right) + \frac{1}{30}h_f \left(\ddot{w}_t' - \ddot{w}_b' \right) \right]$$

$$+ \frac{G_c A_c}{hc^2} \left[-\frac{8}{3} \left(u_t + u_b \right) + \frac{16}{3}u_c \right.$$

$$\left. - \left(\frac{4}{3}h_f + \frac{2}{3}h_c \right) \left(w_t' - w_b' \right) \right] = 0$$

$$\text{(A.4)}$$

$$m_c \left[\frac{2}{105}h_c^2 \ddot{\varphi}_1 + \frac{1}{70}h_c \left(\ddot{u}_t - \ddot{u}_b \right) \right.$$

$$+ \frac{1}{140}h_f h_c \left(\ddot{w}_t' + \ddot{w}_b' \right) \right] + \frac{G_c A_c}{hc^2} \left[-\frac{4}{5}h_c \left(u_t - u_b \right) \right.$$

$$+ \frac{4}{5}h_c^2 \varphi_1 + \frac{4}{15}h_c^2 w_c'$$

$$\left. - \left(\frac{2}{15}h_c^2 + \frac{2}{5}h_c h_f \right) \left(w_t' + w_b' \right) \right] = 0$$
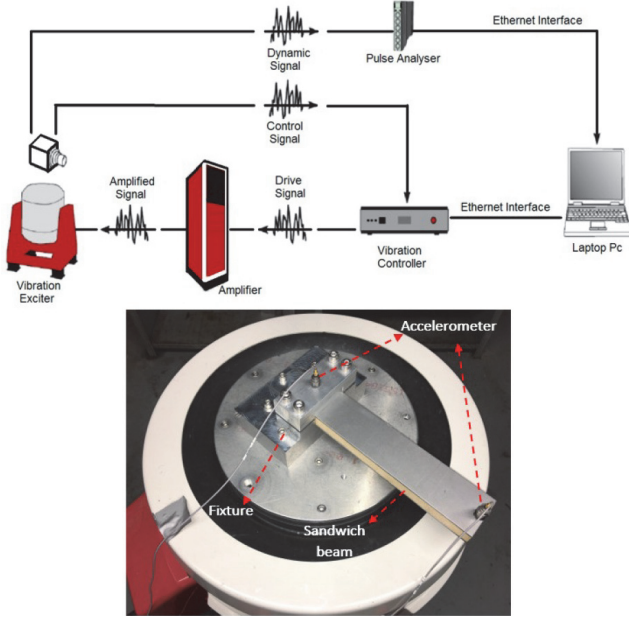
$$\text{(A.5)}$$

FIGURE 8: Schematic of experimental setup.
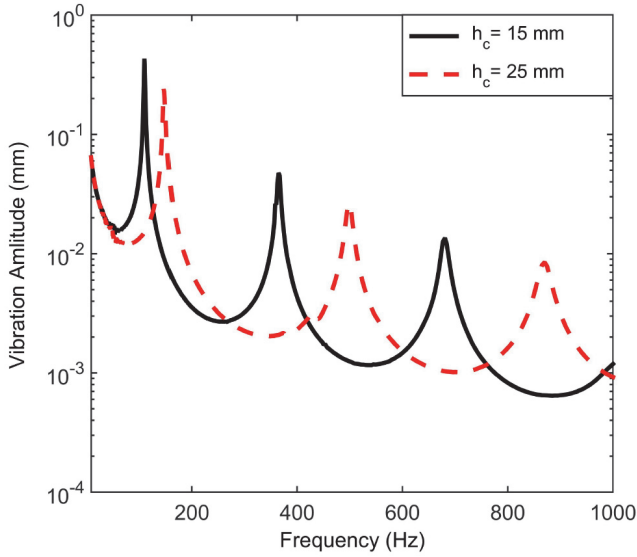

FIGURE 9: Vibration amplitude of cantilever sandwich beam for different core thicknesses by experiment.

$$m_c \left[\frac{8}{15}\ddot{w}_c + \frac{1}{15}h_c \left(\ddot{w}_b + \ddot{w}_t\right) \right]$$
$$+ \frac{G_c A_c}{hc^2} \left[-\frac{2}{5}h_c \left(u'_t - u'_b\right) - \frac{4}{15}h_c^2 \varphi_1 \right.$$
$$\left. - \left(\frac{1}{15}h_f h_c + \frac{1}{15}h_c^2\right)\left(w''_t + w''_b\right) - \frac{8}{15}h_c^2 w''_c \right]$$
$$+ \frac{E_c A_c}{h_c^2} \left[-\frac{8}{3}\left(w_t + w_b\right) + \frac{16}{3}w_c \right] = 0 \tag{A.6}$$

The essential and natural boundary conditions related to the clamped-free case are given as

$$u_t(0,t) = 0,$$
$$P_t(l,t) = 0$$
$$w_t(0,t) = 0,$$
$$V_t(l,t) = 0$$
$$w_{t'}(0,t) = 0,$$
$$M_t(l,t) = 0$$
$$w_c(0,t) = 0,$$
$$V_c(l,t) = 0$$
$$u_b(0,t) = 0,$$
$$P_b(l,t) = 0$$
$$w_b(0,t) = 0,$$
$$V_b(l,t) = 0$$
$$w_{b'}(0,t) = 0,$$
$$M_b(l,t) = 0 \tag{A.7}$$

where the left side of sandwich beam is clamped and the right side is free.

The axial forces $P_{t,b}(x,t)$, the shear forces $V_{t,b,c}(x,t)$, and the bending moments $M_{t,b}(x,t)$ are obtained as

$$P_t = -E_f A_f \frac{\partial u_t}{\partial x} \tag{A.8}$$

$$P_b = -E_f A_f \frac{\partial u_b}{\partial x} \tag{A.9}$$

$$V_t = -\frac{1}{12}m_f h_f^2 \ddot{w}'_t + \frac{m_c}{840}\left[-36h_f \ddot{u}_t - 6h_f \ddot{u}_b \right.$$
$$- 28h_f \ddot{u}_c - 6h_f h_c \ddot{\varphi}_1 + 3h_f^2 \ddot{w}'_b - 18h_f^2 \ddot{w}'_t\right)$$
$$+ E_f I_f w''''_t + \frac{G_c A_c}{840h_c^2}\left[\left(196h_f - 28h_c\right)u_b \right.$$
$$- \left(1316h_f + 532h_c\right)u_t + \left(560h_c + 1120h_f\right)u_c$$
$$+ \left(28h_c^2 - 98h_f^2 + 28h_f h_c\right)w''_b$$
$$- \left(112h_c^2 + 658h_f^2 + 532h_f^2 + 532h_f h_c\right)w'_t$$
$$+ \left(336h_f h_c + 112h_c^2\right)\varphi_1$$
$$- \left(56h_c^2 + 168h_f h_c\right)w'_c\right] \tag{A.10}$$

$$V_b = -\frac{1}{12}m_f h_f^2 \ddot{w}'_b + \frac{m_c}{840}\left(36h_f \ddot{u}_b + 6h_f \ddot{u}_t \right.$$
$$+ 28h_f \ddot{u}_c - 6h_f h_c \ddot{\varphi}_1 + 3h_f^2 \ddot{w}'_t - 18h_f^2 \ddot{w}'_b\right)$$

$$+ E_f I_f w_b'''' + \frac{G_c A_c}{840 h_c^2} \big[\left(-196 h_f + 28 h_c \right) u_t$$

$$+ \left(1316 h_f + 532 h_c \right) u_b - \left(560 h_c + 1120 h_f \right) u_c$$

$$+ \left(28 h_c^2 - 98 h_f^2 + 28 h_f h_c \right) w_t''$$

$$- \left(112 h_c^2 + 658 h_f^2 + 532 h_f^2 + 532 h_f h_c \right) w_b'$$

$$+ \left(336 h_f h_c + 112 h_c^2 \right) \varphi_1$$

$$- \left(56 h_c^2 + 168 h_f h_c \right) w_c' \big] \tag{A.11}$$

$$V_c = \frac{G_c A_c}{840 h_c^2} \big[-336 h_f \left(u_t - u_b \right) - \left(224 h_c^2 \right) \varphi_1$$

$$- \left(56 h_c^2 + 168 h_f h_c \right) \left(w_t' - w_b' \right) - 448 h_c^2 w_c' \big] \tag{A.12}$$

$$M_t = -E_f I_f w_t'' \tag{A.13}$$

$$M_b = -E_f I_f w_b'' \tag{A.14}$$

Data Availability

The data used to support the findings of this study are available from the corresponding author upon request.

Conflicts of Interest

The authors declare that they have no conflicts of interest.

References

[1] A. S. Herrmann, P. C. Zahlen, and I. Zuardy, "Sandwich Structures Technology in Commercial Aviation," in *Proceedings of the 7th International Conference on Sandwich Structures*, pp. 13–26, 2005.

[2] J. Vinson, *The behavior of sandwich structures of isotropic and composite materials*, Technomic Publishing Company, Lancaster, Pennsylvania, 1999.

[3] J. Hohe, L. Librescu, and S. Y. Oh, "Dynamic buckling of flat and curved sandwich panels with transversely compressible core," *Composite Structures*, vol. 74, no. 1, pp. 10–24, 2006.

[4] Y. Frostig and M. Baruch, "Free vibrations of sandwich beams with a transversely flexible core: a high order approach," *Journal of Sound and Vibration*, vol. 176, no. 2, pp. 195–208, 1994.

[5] Y. Frostig, M. Baruch, O. Vilnay, and I. Sheinman, "High-order theory for sandwich-beam behavior with transversely flexible core," *Journal of Engineering Mechanics*, vol. 118, no. 5, pp. 1026–1043, 1992.

[6] O. Rahmani, S. M. R. Khalili, K. Malekzadeh, and H. Hadavinia, "Free vibration analysis of sandwich structures with a flexible functionally graded syntactic core," *Composite Structures*, vol. 91, no. 2, pp. 229–235, 2009.

[7] C. Santiuste, O. T. Thomsen, and Y. Frostig, "Thermo-mechanical load interactions in foam cored axi-symmetric sandwich circular plates - High-order and FE models," *Composite Structures*, vol. 93, no. 2, pp. 369–376, 2011.

[8] R. K. Fruehmann, J. M. Dulieu-Barton, O. T. Thomsen, and S. Zhang, "Experimental investigation of thermal effects in foam cored sandwich beams," in *Thermomechanics and Infra-Red Imaging*, vol. 7 of *Conference Proceedings of the Society for Experimental Mechanics Series*, pp. 83–90, Springer, NY, USA, 2011.

[9] V. S. Sokolinsky and S. R. Nutt, "Consistent Higher-Order Dynamic Equations for Soft-Core Sandwich Beams," *AIAA Journal*, vol. 42, no. 2, pp. 374–382, 2004.

[10] Y. Frostig, C. Phan, and G. Kardomateas, "Free vibration of unidirectional sandwich panels, Part I: Compressible core," *Journal of Sandwich Structures and Materials*, vol. 15, no. 4, pp. 377–411, 2013.

[11] A. R. Damanpack and S. M. R. Khalili, "High-order free vibration analysis of sandwich beams with a flexible core using dynamic stiffness method," *Composite Structures*, vol. 94, no. 5, pp. 1503–1514, 2012.

[12] M. Yang and P. Qiao, "Higher-order impact modeling of sandwich structures with flexible core," *International Journal of Solids and Structures*, vol. 42, no. 20, pp. 5460–5490, 2005.

[13] Y. Wang and X. Wang, "Free vibration analysis of soft-core sandwich beams by the novel weak form quadrature element method," *Journal of Sandwich Structures and Materials*, vol. 18, no. 3, pp. 294–320, 2015.

[14] X. Wang and X. Liang, "Free vibration of soft-core sandwich panels with general boundary conditions by harmonic quadrature element method," *Thin-Walled Structures*, vol. 113, pp. 253–261, 2017.

[15] F. Tornabene, N. Fantuzzi, and M. Bacciocchi, "The local GDQ method applied to general higher-order theories of doubly-curved laminated composite shells and panels: the free vibration analysis," *Composite Structures*, vol. 116, pp. 637–660, 2014.

[16] C. C. Hong, H. W. Liao, L. T. Lee, J. B. Ke, and K. C. Jane, "Thermally induced vibration of a thermal sleeve with the GDQ method," *International Journal of Mechanical Sciences*, vol. 47, no. 12, pp. 1789–1806, 2005.

[17] H. D. Chalak, A. Chakrabarti, M. A. Iqbal, and A. H. Sheikh, "Vibration of laminated sandwich beams having soft core," *Journal of Vibration and Control*, vol. 18, no. 10, pp. 1422–1435, 2012.

[18] K. M. Ahmed, "Free vibration of curved sandwich beams by the method of finite elements," *Journal of Sound and Vibration*, vol. 18, no. 1, pp. 61–74, 1971.

[19] N. Nanda, S. Kapuria, and S. Gopalakrishnan, "Spectral finite element based on an efficient layerwise theory for wave propagation analysis of composite and sandwich beams," *Journal of Sound and Vibration*, vol. 333, no. 31, pp. 20–27, 2014.

[20] Y. Pourvais, P. Asgari, A. R. Moradi, and O. Rahmani, "Experimental and finite element analysis of higher order behaviour of sandwich beams using digital projection moiré," *Polymer Testing*, vol. 38, pp. 7–17, 2014.

[21] R. Long, O. Barry, and D. C. D. Oguamanam, "Finite element free vibration analysis of soft-core sandwich beams," *AIAA Journal*, vol. 50, no. 1, pp. 235–238, 2012.

[22] W. L. Chen, A. G. Striz, and C. W. Bert, "High-accuracy plane stress and plate elements in the quadrature element method," *International Journal of Solids and Structures*, vol. 37, no. 4, pp. 627–647, 2000.

[23] Y. Xing and B. Liu, "High-accuracy differential quadrature finite element method and its application to free vibrations of thin plate with curvilinear domain," *International Journal for*

Numerical Methods in Engineering, vol. 80, no. 13, pp. 1718–1742, 2009.

[24] Y. Wang and X. Wang, "Static analysis of higher order sandwich beams by weak form quadrature element method," *Composite Structures*, vol. 116, no. 1, pp. 841–848, 2014.

[25] F. Tornabene, S. Brischetto, N. Fantuzzi, and M. Bacciocchi, "Boundary conditions in 2D numerical and 3D exact models for cylindrical bending analysis of functionally graded structures," *Shock and Vibration*, vol. 2016, Article ID 2373862, 2016.

[26] F. Tornabene, N. Fantuzzi, and M. Bacciocchi, "The GDQ method for the free vibration analysis of arbitrarily shaped laminated composite shells using a NURBS-based isogeometric approach," *Composite Structures*, vol. 154, pp. 190–218, 2016.

[27] Z. Zong and Y. Zhang, *Advanced differential quadrature methods*, CRC Press, NY, USA, 2009.

[28] N. A. Rubayi and S. Charoenree, "Natural frequencies of vibration of cantilever sandwich beams," *Computers & Structures*, vol. 7, no. 6, pp. 737–745, 1977.

[29] M. Azimi, M. Shahravi, and E. F. Joubaneh, "Dynamic analysis of maneuvering flexible spacecraft appendage using higher order sandwich panel theory," *Latin American Journal of Solids and Structures*, vol. 13, no. 2, pp. 296–313, 2016.